

An integrated approach to the characterization of powder metallurgy components performance during green machining

Etienne Robert-Perron^{a,*}, Carl Blais^a, Yannig Thomas^b, Sylvain Pelletier^b, Martin Dionne^c

^a *Department of Mining, Metallurgical and Materials Engineering, Université Laval, Pavillon Adrien Pouliot, Room 1728, Quebec City, QC, Canada G1K 7P4*

^b *Powder Forming Research Group, Industrial Materials Institute – National Research Council, Boucherville, QC, Canada*

^c *Quebec Metal Powders Ltd., Sorel-Tracy, QC, Canada*

Received in revised form 18 April 2005; accepted 11 May 2005

Abstract

Green machining of powder metallurgy (P/M) components appears as an interesting procedure to solve the eternal problems associated with the poor machining behaviour of porous metallic samples. With the increasing usage of sinter-hardenable powders for high performance applications, green machining is an attractive method to lower production costs and compete against other shaping processes. Green machining is not a straightforward procedure. There is quite more to control in green machining than the cutting parameters. Several variables must be optimized to obtain adequate results in terms of surface finish, geometrical conformance and productivity. Other considerations such as density gradients in green compacts also influence the final outcome of this process. This study presents a new technique, based on cutting force measurements during green turning, to quickly and precisely characterize density gradients in powder metallurgy components. This new technique also allows the characterization of green machinability. Moreover, this study shows that timing sprockets can be produced by green machining of gear blanks. Timing sprockets produced by this process show a surface finish comparable to that of powder metallurgy components machined after sintering.

© 2005 Elsevier B.V. All rights reserved.

Keywords: Powder metallurgy; Green machining; Sinter-hardening; Green strength; Density gradients; Binder; Lubricant

1. Introduction

Powder metallurgy (P/M) is a near-net shape process that tends to eliminate the necessity of secondary shaping operations. However, features such as holes perpendicular to the pressing axis, undercuts and threads generally necessitate the use of machining operations [1]. Unfortunately, P/M components are difficult to machine due to their internal porosity, which induces microvibrations in the cutting tool and lowers the thermal conductivity of the material [2]. The machining of sinter-hardenable components is even more difficult since those samples exhibit hard microstructures (martensite + bainite). During the machining of such components, the temperature at the tool/chip interface increases significantly and the cutting tool life is considerably reduced.

A prospective avenue to improve the machining performances of P/M components is green machining. Green machining implies that the machining operations are done while the parts are in their “green state”, before sintering. The advantages of this approach are impressive: tool wear becomes a negligible factor since the cutting forces applied on the tool are small and heat generation is minimal; the harder and/or tougher phases that are needed to obtain improved mechanical properties have not yet been formed since phase transformation only occurs at the end of the sintering operation. Thus, the productivity can be significantly increased because down time due to tool replacement is kept to a minimum. Nevertheless, important obstacles have to be addressed. The green strength of P/M components is generally low. For example, steel parts pressed to a green density of 6.8 g/cm³ usually show green strength values of 12–17 MPa (~1750–2500 psi). Therefore, the potential gains described above can easily be offset by the weak mechanical

* Corresponding author.

E-mail address: etienne.robert-perron.1@ulaval.ca (E. Robert-Perron).

resistance of the green parts. The latter characteristic leads to poor surface finish, chipped or broken edges and sometimes broken parts. However, recent advancements in parts manufacturing as well as binder/lubricant technology open new leads in the development of green machining of P/M components. One method to make green machining possible is warm compaction [3–7]. This technique consists in pressing a pre-heated powder in a heated die at a temperature typically ranging from 90 to 150 °C. The green strength obtained from this approach is about two times larger than that provided by cold compaction [8]. Another option is the use of new binder/lubricant systems that have been developed to increase the green strength of P/M components without requiring heated compaction tooling. These polymeric binder/lubricant systems also offer the possibility of further strengthening the components by performing a curing treatment at approximately 175 °C following compaction [9–13]. The latter approach permits to increase the green strength of P/M components by a factor of 2–3. With such high green strength values, it is believed that green machining could be used to increase the productivity of the P/M process. Therefore, green machining could open up new fields of applications in powder metallurgy. Until now, P/M parts with hard microstructures were often judged too difficult to be machined. However, with the development of improved binder/lubricant systems, it appears possible to perform machining in the green state and then sinter the parts to obtain the microstructure needed for the given mechanical properties.

It is well established that green density influences green strength [10–12]. A high green density, due to a high compacting stress, promotes increased particle movement and deformation, which are the bases for cold welding, mechanical interlocking and increased green strength [14]. However, due to non-uniform stress distribution during compaction, density gradients may be induced in green compacts. Die displacement during compaction as well as friction between particles and die wall are the main causes of pressure gradients that lead to the occurrence of density gradients. In double action pressing, the area with the lowest density is usually located near the mid-height of the component [2]. Thus, green strength gradients must also exist in a component with density gradients. Moreover, the cutting forces involved during machining are strongly influenced by the strength of the material [15]. If density gradients lead to green strength gradients, it will presumably lead to variations of the cutting forces applied on the tool during green machining. These cutting force gradients should vary in a similar way with the density gradients. In addition, machinability of green components, in terms of surface finish, is function of green strength. Since green strength varies within a green component, surface finish after green machining should vary accordingly.

The objective of this study was the development of a new technique to characterize density gradients in P/M components and its application to green machining evaluation. An

investigation performed on gears in their green state was also conducted to simulate the machining of timing sprockets. This practical investigation was done to evaluate the effect of a curing treatment on the green machinability of high green strength compacts and to optimize the cutting parameters for surface finish.

2. Experimental procedures

2.1. Sample pressing

One series of samples was produced based on Quebec Metal Powders 4601 sinter-hardenable powder (Fe-1.8 wt% Ni, 0.55 wt% Mo and 0.2 wt% Mn) to which was added 2.0 wt% Cu and 0.6 wt% C. The latter premix follows the denomination FLC-4608 of MPIF [16]. Lubrication was done using 0.75 wt% of ethylenebisstearamide (EBS). Samples were pressed, using a 150-tonnes mechanical press (Gasbarre Products Inc.) into rings (50.8 mm o.d., 19.0 mm i.d. and 19.0 mm in height) to a green density of 6.80 g/cm³. The compaction of these samples was done at a tool temperature of 53 °C, which is the typical temperature reached without external heating. The rings were used for the development of a new technique to characterize density gradients in P/M components. This new technique also allows the characterization of the green machinability based on the density gradients.

Other series of samples were prepared from a premix having the same chemistry described earlier and admixed either with 0.75 wt% EBS (reference material) or 0.65 wt% of a new binder/lubricant (FLOMET HGSTM) specifically developed for high green strength. These two mixes of powders were pressed into gears (15 teeth, 50.8 mm o.d., 12.7 mm i.d. and 12.7 mm in height) at four different densities 6.60, 6.80, 7.00 and 7.20 g/cm³. The compaction of these samples was done using a tool temperature of 65 °C, which is the typical temperature reached during pressing samples of this geometry without external heating. The gear-shaped samples were used for the simulation of the machining of timing sprockets in their green state. Finally, since the FLOMET HGSTM system offers the possibility of further strengthening the components through a curing treatment, half of the samples produced were subjected to such a treatment, which consists in heating the parts in air at 175 °C for 1 h.

2.2. Sample holding for turning operations

A special fixture was developed to prevent the damage of the green P/M parts while held in the chuck of the lathe (Fig. 1). The samples had a hole in the middle and they were fixed to a wrought steel bar using a screw and a tight fitting bushing (Fig. 1). Thus, the steel bar was placed in the chuck of the lathe, preventing the jaws of the chuck from touching the P/M components. The turning was performed on a Mazak Nexus 100 CNC lathe.

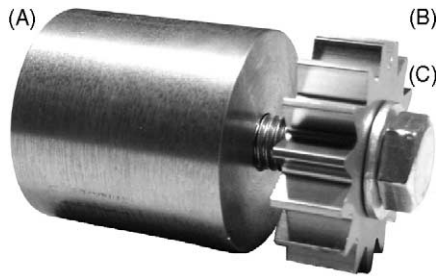


Fig. 1. Sample holder developed for green machining: (A) steel bar fixed in the chuck of the lathe to hold the sample, (B) sample to be machined and (C) tightening screw used to fix the sample on the steel bar.

2.3. Characterization of the machining performances

The machinability criterion used in this study was edge integrity based on the average width of breakouts formed near the edges of machined surfaces. Those breakouts are formed by particle removal during machining. For rings, 25 measurements were performed on the edges of freshly machined surfaces using an image analysis routine in optical microscopy. For gears, the measurements were performed only on the outlet edge of machined teeth, defined as the last edge seen by the cutting tool as it moves from one tooth to the other. Measurements along the inlet edge, defined as the edge initially in contact with the tool as it starts cutting each tooth, were neglected since the width of the breakouts in that area was judged negligible. Fig. 2 summarizes the image analysis procedure that was developed. The dark region in Fig. 2A corresponds to the area, where powder particles were removed during green machining. Fig. 2B shows an example of the measurements performed by the image analysis system to measure the average width of the breakout area. Although the breakouts shown in Fig. 2 seem to penetrate deeply inside the tooth, their typical depth is approximately equal to one-third of their width as highlighted in Fig. 3.

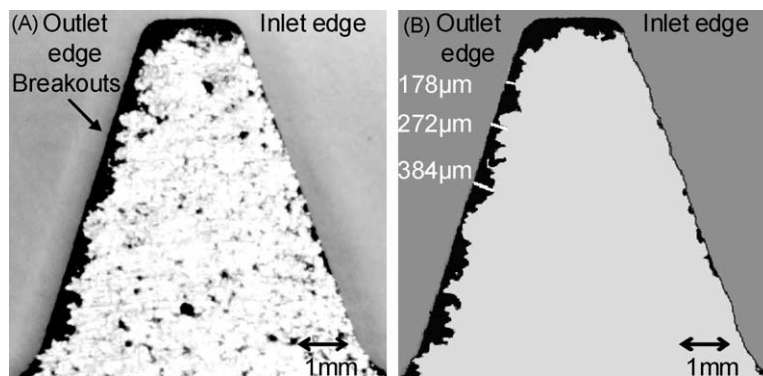


Fig. 2. Typical micrograph of a gear tooth after green machining. Dark surface corresponds to areas where particles were removed by the passage of the cutting tool. (A) Original micrograph (optical microscopy-unpolished, unetched) and (B) typical result obtained with the image analysis routine developed. Average width of breakout is 255 μm .

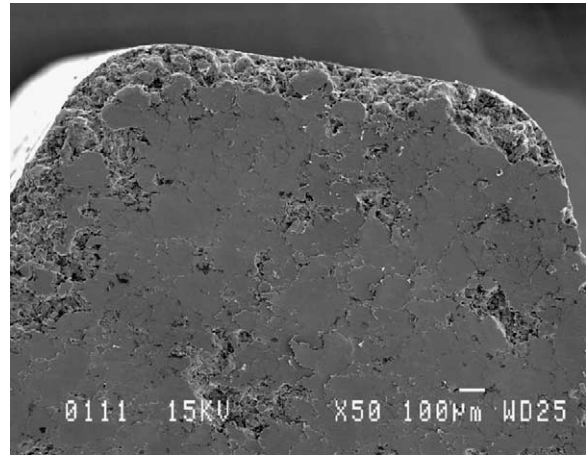


Fig. 3. SEM micrograph of a typical tooth showing a depth of the breakouts approximately one-third of its width.

2.4. Characterization of density gradients

Characterization of density gradients was initially performed by slicing several rings along the pressing axis. This technique was used to establish a reference with which to compare the results obtained with the new technique. The cross-sections were prepared for optical microscopy using vacuum resin impregnation followed by polishing. Image analysis in optical microscopy was performed on the entire surface of the sections, and the volume fraction of porosity was measured. The latter approach allowed identifying the presence of porosity gradients, which were interpreted as density gradients. The remaining samples were used to measure the cutting force gradients during green machining. The machining operation selected for measuring cutting force gradients was the turning of grooves. Turning of a groove is defined by only two cutting parameters (surface speed and feed rate), being easier to control than conventional turning, which requires the setting of a third parameter, the depth of cut. A series of grooves having a width of 1.6 mm and a depth

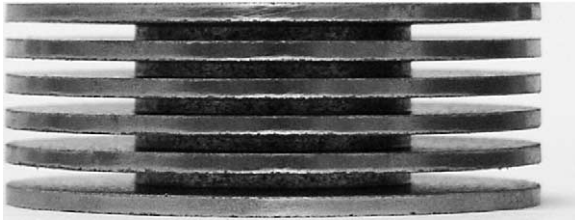


Fig. 4. Example of a machined test piece used to characterize variations of cutting forces during green turning.

of 12.7 mm were machined along the radial axis of each ring (Fig. 4). The force acting on the cutting tool was measured using a Kistler dynamometer. Machining was performed at a cutting speed of 152 m/min and a feed rate of 0.0254 mm/rev. The cutting tool used for this operation was a SGFH 19-1 manufactured by ISCAR. Finally, each ring was sliced in half along the middle of its groove and the machined surfaces were characterized in optical microscopy. The average width of breakouts was measured on each surface to determine the effect of density gradients on machinability. The results obtained are presented in the next section.

2.5. Green machining experiments in interrupted cutting

The machining operation performed on gears in their green state was the turning of a groove of 6 mm wide and 8 mm deep (Fig. 5) to simulate the machining of timing sprockets. This type of machining is defined as interrupted cutting due to the jump from one tooth to another. The cutting tool used for this operation was a GIP6.00E-0.80 IC-9015 manufactured by ISCAR. This cutter was selected so it would require only one cut to produce the desired groove (6 mm wide). There are two cutting parameters when turning a groove: the surface speed and the feed rate. In addition, the influence of the density

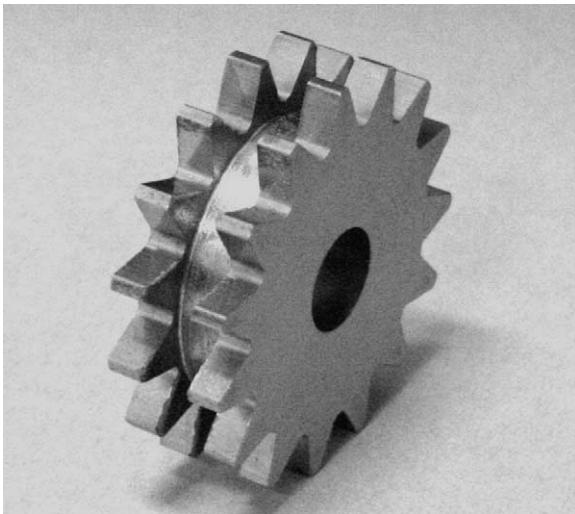


Fig. 5. Result obtained after machining a groove in the middle of a part similar to that of Fig. 1 simulating the manufacturing of a timing sprocket.

Table 1

Cutting parameters and levels investigated for the machining of timing sprockets

| Parameters | Levels | | | |
|------------------------------|--------|--------|--------|--------|
| | 1 | 2 | 3 | 4 |
| Density (g/cm ³) | 6.60 | 6.80 | 7.00 | 7.20 |
| Surface speed (m/min) | 152 | 305 | 457 | 610 |
| Feed rate (mm/rev.) | 0.0051 | 0.0127 | 0.0254 | 0.0508 |

of the components was investigated in this study. Table 1 summarizes the ranges of parameters investigated.

Since the test matrix involved 64 experiments for each of the three investigated systems (EBS, FLOMET HGSTM as-pressed and FLOMET HGSTM cured), a design of experiment using orthogonal arrays and signal-to-noise (S/N) ratios was used [17,18]. Using design of experiment, only 16 tests (array L₁₆) were needed to obtain significant results while allowing the determination of the relative influence of each parameter studied. This array makes separation of any of the main parameter effects and interactions impossible. Using such an array assumes that there is no interaction between the parameters studied. This approach was selected because the parameters analyzed were operation based, and therefore judged mutually independent [17,19].

3. Results and discussion

3.1. Characterization of density gradients by a quick machining procedure

3.1.1. Correlation between density gradients and cutting forces

Fig. 6 compares the evolution of porosity gradients measured by image analysis (Fig. 6A) with the variation of the cutting forces measured with a dynamometer during green machining of rings (Fig. 6B). Comparison of the two profiles clearly indicates that there is a correlation between the two sets of results. As it was anticipated, the cutting forces are sensitive to small variations in green strength, and therefore green density. As seen, image analysis showed that there was a low-density area located at approximately two-third of the height of the component when starting from the bottom (arrow 1, Fig. 6A). Similarly, the dynamometer recorded lower cutting forces in the same area confirming that density gradients lead to cutting force gradients during machining. These results indicate that a dynamometer can be used to determine the location of green density gradients. This new technique of characterizing green density gradients is significantly less time consuming than the established method based on image analysis. Thus, it can be used during press set up to optimize die filling as well as tooling movement to minimize green density gradients and/or to optimize the location of low-density areas within the green components. Furthermore, it can be assumed that the proposed approach

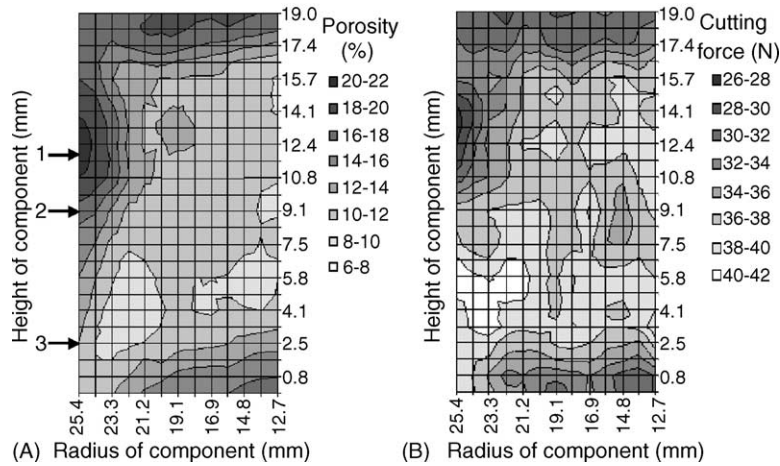


Fig. 6. (A) Typical porosity gradient in the green components studied. (B) Typical cutting forces gradient measured during green machining (forces in Newton).

is at least as accurate as the conventional technique since it does not involve sample preparation procedures such as mounting and polishing. Thus, the risks of particle removal due to sample preparation are kept to a minimum.

3.1.2. Effect of the density gradient on green machining

Fig. 7 presents micrographs of machined surfaces (walls of the grooves) taken at different locations along the height of the component (corresponding to the arrows in Fig. 6A). These micrographs show that variations in green density significantly influence the surface finish of components machined in green state. The micrograph presented in Fig. 7A shows that when a groove is machined in an area with a rather high percentage of porosity (arrow 1 in Fig. 6A), edge integrity is severely affected. As the machining operation is performed in areas presenting lower percentage of porosity (arrows 2 and 3 in Fig. 6A), edge integrity improves accordingly, as shown in Fig. 7B and C. Thus, the new characterization technique presented above not only allows the quantitative characterization of green density gradients in P/M components, but can also be used to predict the surface finish in green machining.

3.2. Green machining experiments in interrupted cutting

3.2.1. Characterization of the green strength

Fig. 8 presents the green strength values, measured according to MPIF Standard 15 [20], as function of the green density for the three systems investigated for the production of gears. There is a strong improvement of the green strength by using

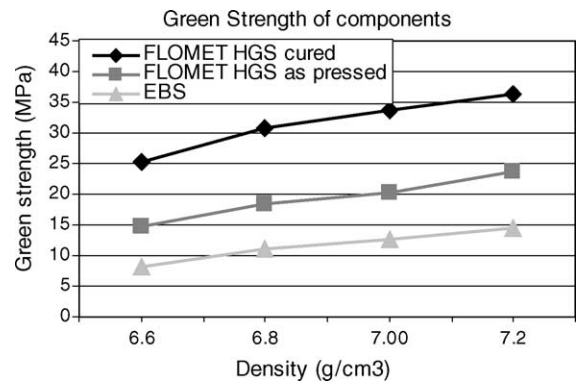


Fig. 8. Variation of the green strength of the three series of P/M components as a function of green density.

the system FLOMET HGS binder/lubricant. Moreover, these values can be increased by typically 70% by performing a curing treatment. The latter system exhibits green strengths more than twice higher than the EBS system. This improvement is explained by the ability of the polymeric binder/lubricant to flow through the porosities during the curing treatment and create a strong continuous polymeric network that strengthens the components [12].

3.2.2. Characterization of density gradients in the gears

As shown previously, conducting green machining experiments involves first, the characterization of density gradients in green compacts. In the gears studied, there was not only a typical density gradient in the direction of the pressing axis

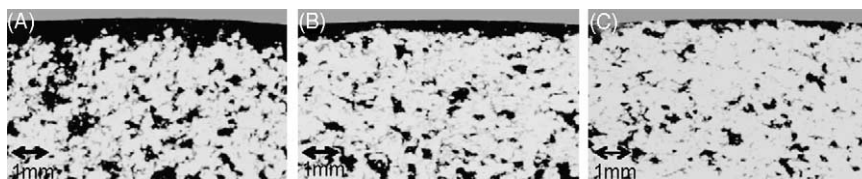


Fig. 7. Micrographs of the machined surfaces from different areas arrowed in Fig. 6. (A) area corresponding to arrow 1, (B) area corresponding to arrow 2 and (C) area corresponding to arrow 3 (optical microscopy-unpolished, unetched).

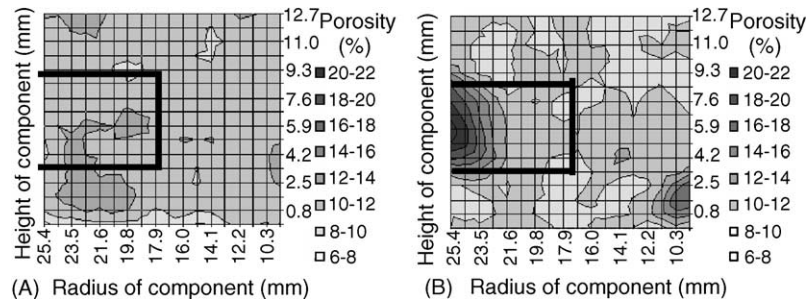


Fig. 9. (A) Typical porosity gradients on tooth A. (B) Typical porosity gradients on tooth E.

but also a circumferential density gradient. Therefore, the green density as well as the green strength and green machinability varied circumferentially in gears from one tooth to another. This behaviour is assumed to stem from improper die filling. The circumferential density gradient in gears was characterized by vertically slicing a gear in the middle of each tooth, and then performing image analysis routines on the entire cross-sections of all the teeth of the gear. Following this procedure, porosity gradients on each tooth was obtained, which allow the characterization of the circumferential porosity gradient.

Fig. 9A presents porosity gradients on the cross-section of tooth A, having the lowest percentage of porosity, while Fig. 9B presents porosity gradients on the cross-section of tooth E, having the highest percentage of porosity. Both figures are obtained from the same gear, at a density of 7.20 g/cm^3 . It is clearly shown in Fig. 9 that porosity gradients exist on the gears studied not only in the direction of the pressing axis, but also circumferentially. There is no porosity gradient in tooth A while there is a distinguishable porosity gradient in tooth E. The dark rectangles on both figures represent the area where the machining operation (turning of a groove) is performed. It is important to note that the characterization work was performed on several gears and all results showed tooth A always having the lowest percentage of porosity while tooth E the highest percentage of porosity.

Fig. 10A shows a typical micrograph of the internal machined surface of tooth A and Fig. 10B of the machined

surface of tooth E. Both figures are from the same component (system FLOMET HGS as-pressed: density of 7.20 g/cm^3 , surface speed of 152 m/min and feed rate of 0.0254 mm/rev.) As predicted, the circumferential porosity gradient affects the green machinability of a component from one tooth to another. The average length of breakouts is 36% larger for tooth E ($362 \mu\text{m}$) than for tooth A ($266 \mu\text{m}$). This observation is attributed to the lower green strength of tooth E compared to tooth A.

3.2.3. Optimization of cutting parameters in interrupted cutting: turning of a groove

The first system investigated was the EBS system. For this system, regardless of the cutting conditions, the average length of breakouts was always over a $1000 \mu\text{m}$. Fig. 11 presents a typical micrograph obtained from an internal machined surface of an average tooth. As can be seen, almost 50% of the surface has been damaged during the machining operation and the average length of breakouts is $1100 \mu\text{m}$. The gears produced from the EBS system exhibited poor green machinability in interrupted cutting due to their low-green strength. Thus, the optimization of cutting parameters for this system was judged irrelevant.

The second system investigated was the FLOMET HGS as-pressed. The results for this set of samples, in term of average length of breakouts, are shown in Table 2. Note that the results for experiments #1 and #8 are over a $1000 \mu\text{m}$;

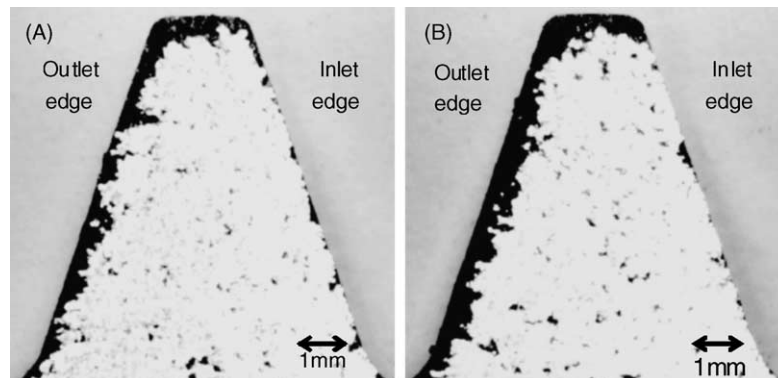


Fig. 10. (A) Typical micrograph obtained for tooth A. (B) Typical micrograph obtained for tooth E.

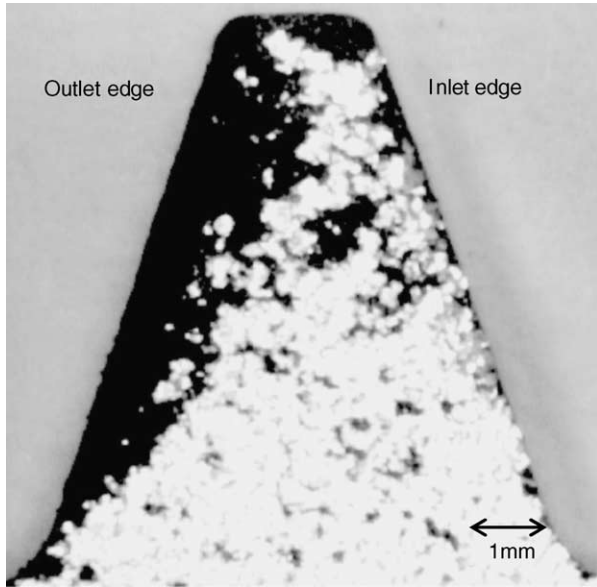


Fig. 11. Typical micrograph obtained for the EBS system in green machining.

therefore, these two values were not considered in the data analysis.

The primary goal of using a test matrix was to optimize the outcome of the green machining process, that is, to determine the optimum conditions for each parameter. This was achieved by taking the numerical values of S/N ratio, listed

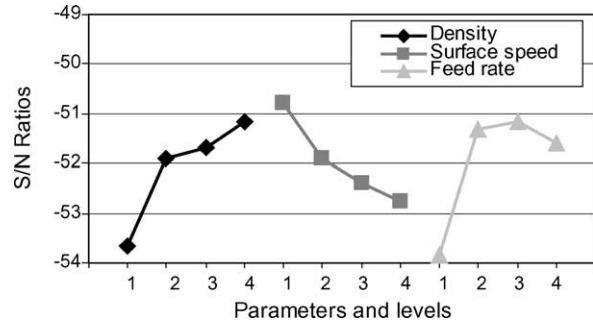


Fig. 12. Graph of parameters effects for the gears from the system FLOMET HGS as-pressed.

in Table 2, and averaging them by parameter levels, as shown in Table 3. These averages are shown graphically in Fig. 12. The latter shows that each parameter reaches an optimum level (closest value to zero). Therefore, the optimum cutting conditions for turning a groove in interrupted cutting for the gears from the system FLOMET HGS as-pressed are density of 7.20 g/cm³, surface speed of 152 m/min and feed rate of 0.0254 mm/rev. To estimate the effect of the three machining parameters, an analysis of variance (ANOVA) was performed [17]. The results are presented in Table 3. It is shown that the density contributes for 40%, the feed rate for 37% and the surface speed for 23% of the variation of the length of breakouts.

As anticipated, the components having high density showed higher machinability since their green strength was

Table 2
Test matrix (L₁₆) and average length of breakouts for the FLOMET HGS system in as-pressed conditions

| Experiment | Parameters and levels | | | Average length of breakouts (μm) | S/N ratios |
|------------|-----------------------|---------------|-----------|----------------------------------|------------|
| | Density | Surface speed | Feed rate | | |
| 1 | 1 | 1 | 1 | >1000 | <-60.00 |
| 2 | 1 | 2 | 4 | 420 | -52.46 |
| 3 | 1 | 3 | 3 | 419 | -52.44 |
| 4 | 1 | 4 | 2 | 636 | -56.07 |
| 5 | 2 | 1 | 4 | 401 | -52.06 |
| 6 | 2 | 2 | 3 | 362 | -51.17 |
| 7 | 2 | 3 | 2 | 418 | -52.42 |
| 8 | 2 | 4 | 1 | >1000 | <-60.00 |
| 9 | 3 | 1 | 3 | 325 | -50.24 |
| 10 | 3 | 2 | 2 | 339 | -50.60 |
| 11 | 3 | 3 | 1 | 519 | -54.30 |
| 12 | 3 | 4 | 4 | 377 | -51.53 |
| 13 | 4 | 1 | 2 | 320 | -50.10 |
| 14 | 4 | 2 | 1 | 468 | -53.40 |
| 15 | 4 | 3 | 4 | 329 | -50.34 |
| 16 | 4 | 4 | 3 | 345 | -50.76 |

Table 3
Average S/N ratios and analysis of variance as a function of parameter levels for the gears from the FLOMET HGS system in as-pressed conditions

| Parameters | Levels | | | | Sum of squares | Relative influence (%) |
|---------------|--------|--------|--------|--------|----------------|------------------------|
| | 1 | 2 | 3 | 4 | | |
| Density | -53.66 | -51.89 | -51.67 | -51.15 | 11.6 | 40 |
| Surface speed | -50.80 | -51.91 | -52.38 | -52.78 | 6.8 | 23 |
| Feed rate | -53.85 | -51.30 | -51.15 | -51.60 | 10.7 | 37 |

Table 4

Feed force measured during green machining of a component (density 7.20 g/cm³) at different feed rates

| Cutting speed (m/min) | Feed rate (mm/rev.) | Feed force (N) |
|-----------------------|---------------------|----------------|
| 305 | 0.0254 | 35.9 |
| | 0.0508 | 46.7 |

higher. In Fig. 12, it can be seen that the optimum feed rate is not the lowest one. This can be explained by the relatively high temperature (~55 °C) reached during green machining. At low-feed rates, the time required to machine the component increases leading to an increase of the temperature of the component. Therefore, the binder/lubricant loses its mechanical properties, and the green strength of the component decreases promoting particles removal during machining. At high feed rates (0.0508 mm/rev.), particles also have the tendency of being removed since the feed forces acting on the part are high, as shown in Table 4. Thus, the bonds between particles and binder/lubricant cannot support such high forces and particles are removed.

Finally, it is possible to predict the average length of breakouts using the optimum cutting conditions. Therefore, for a component manufactured with the FLOMET HGS system in as-pressed conditions, the average length of breakouts predicted by the model is 286 μm using the above optimum conditions. However, the experimental average length of breakouts is 315 μm (Fig. 13). There is a 10% error between the prediction of the model and experimental results.

The last system investigated was the FLOMET HGS cured. Table 5 shows the results for this system, in terms of average length of breakouts for the different conditions.

Once again, the determination of the optimum level for each parameter was obtained by taking the numerical values of S/N ratio, listed in Table 5 and averaging them by parameter levels, as shown in Table 6. These averages are shown graphically in Fig. 14. Therefore, the optimum cutting

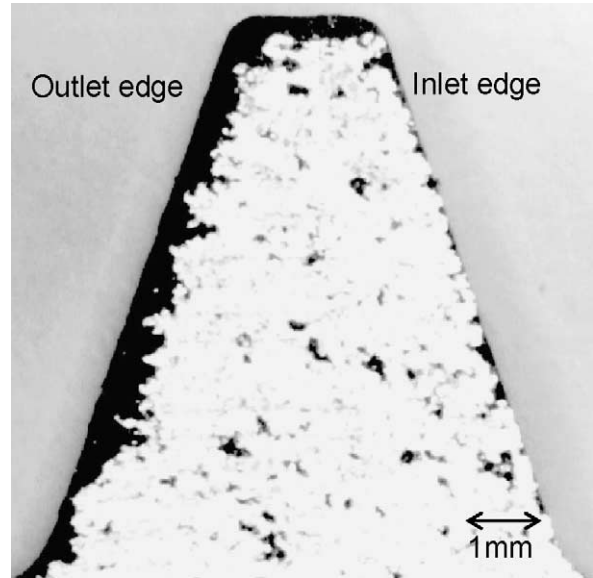


Fig. 13. Typical micrograph from the system FLOMET HGS as-pressed machined under the optimum cutting conditions.

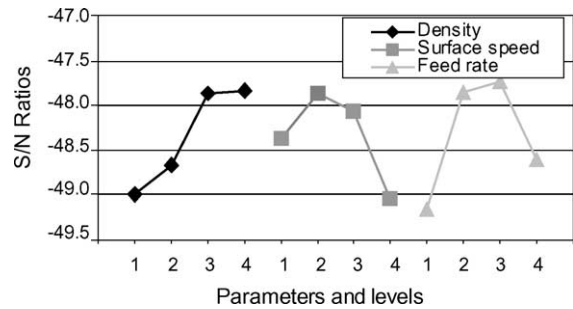


Fig. 14. Graph of parameter effects for the system FLOMET HGS cured.

Table 5

Matrix experiment (L₁₆) and average length of breakouts for the system FLOMET HGS cured

| Experiment | Parameters and levels | | | Average length of breakouts (μm) | S/N ratios |
|------------|-----------------------|---------------|-----------|----------------------------------|------------|
| | Density | Surface speed | Feed rate | | |
| 1 | 1 | 1 | 1 | 308 | -49.77 |
| 2 | 1 | 2 | 4 | 284 | -49.07 |
| 3 | 1 | 3 | 3 | 270 | -48.63 |
| 4 | 1 | 4 | 2 | 266 | -48.50 |
| 5 | 2 | 1 | 4 | 259 | -48.27 |
| 6 | 2 | 2 | 3 | 245 | -47.80 |
| 7 | 2 | 3 | 2 | 236 | -47.46 |
| 8 | 2 | 4 | 1 | 360 | -51.13 |
| 9 | 3 | 1 | 3 | 226 | -47.08 |
| 10 | 3 | 2 | 2 | 225 | -47.04 |
| 11 | 3 | 3 | 1 | 257 | -48.20 |
| 12 | 3 | 4 | 4 | 286 | -49.13 |
| 13 | 4 | 1 | 2 | 263 | -48.40 |
| 14 | 4 | 2 | 1 | 238 | -47.53 |
| 15 | 4 | 3 | 4 | 250 | -47.96 |
| 16 | 4 | 4 | 3 | 235 | -47.42 |

Table 6
Average S/N ratio by parameter levels and analysis of variance for system FLOMET HGS cured

| Parameters | Levels | | | | Sum of squares | Relative influence (%) |
|---------------|--------|--------|--------|--------|----------------|------------------------|
| | 1 | 2 | 3 | 4 | | |
| Density | −48.99 | −48.66 | −47.86 | −47.83 | 4.1 | 32 |
| Surface speed | −48.38 | −47.86 | −48.06 | −49.04 | 3.2 | 25 |
| Feed rate | −49.16 | −47.85 | −47.73 | −48.60 | 4.4 | 43 |

conditions for turning of a groove in interrupted cutting for gears from the system FLOMET HGS cured are density of 7.20 g/cm^3 , surface speed of 305 m/min and feed rate of 0.0254 mm/rev . An analysis of variance was performed to estimate the effect of the machining parameters on the green machinability of the gears from the system FLOMET HGS cured, as shown in Table 6. Therefore, the feed rate weights for 43%, the density for 32% and the surface speed for 25% of the variation of the length of breakouts. These results are similar to those obtained with the gears from the system FLOMET HGS as-pressed. However, the optimum surface speed for the system FLOMET HGS cured is not the lowest one. At the lower surface speed, the machining time is very long and the temperature of the components reached 65°C , which affects severely the green strength of the parts. Higher temperature is reached during machining of the cured system since the green strength of these parts is higher. On the other hand, as said previously, the highest feed rate promotes particles removal since the cutting force increases.

It is possible to predict the average length of breakouts using the optimum cutting conditions. For a gear from the system FLOMET HGS cured, machined under the above optimum conditions, the average length of breakouts predicted is $217 \mu\text{m}$. The experimentally measured average length of breakout was $220 \mu\text{m}$ (Fig. 15). There is a 1% error between

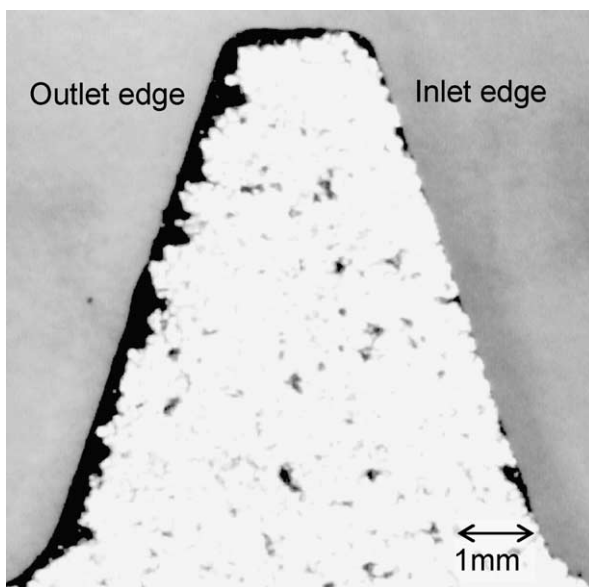


Fig. 15. Typical micrograph from the system FLOMET HGS cured, machined under the optimum cutting conditions.

the predictions of the model and reality, which is very small due to the relatively small variance of the results (13%). A larger error (10%) was obtained for the as-pressed system since the variance of the results was larger (22%). Furthermore, since the surface speed has the lowest influence on the variation of the green machinability (25%) and the difference between the average S/N ratio for levels two and three is very small, this parameter can be increased without affecting severely the result. If the surface speed is increased from 305 to 457 m/min (50% higher), the average length of breakouts predicted by the model is increased to $223 \mu\text{m}$, which is only 4% longer.

3.3. Comparison with sintered components

The results presented in the previous sections indicate the advantage of using the FLOMET HGS system after a curing treatment for a green machining process. There is a reduction of 36% in the average length of breakouts by machining cured parts. In order to evaluate correctly the quality of the machined surfaces obtained by green machining, a comparison with a component machined after sintering was performed. Fig. 16 presents a typical micrograph (SEM) of an outlet edge of a machined tooth. The micrograph shows the presence of burrs that smeared beyond the edge of the tooth. The average length of the burrs is $200 \mu\text{m}$, which is in the same range as the average width of the breakouts ($220 \mu\text{m}$) observed after green machining. Therefore, green machining provides a similar edge integrity to a sintered component.

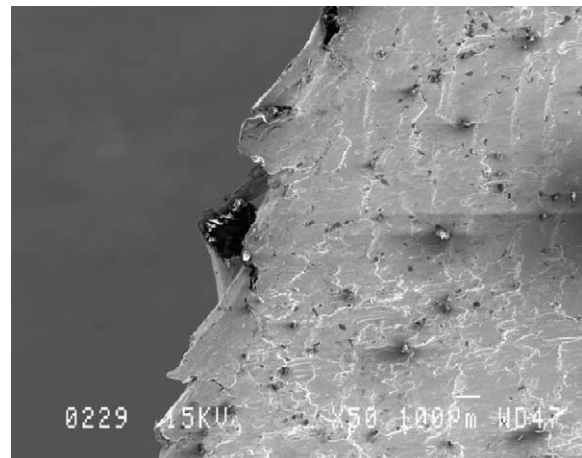


Fig. 16. Typical micrograph obtained after machining a sintered component.

4. Conclusions

The study investigated the characterization and the optimization of green machining of P/M steel components. The main findings of the research are summarized below:

- It has been demonstrated that high quality components can be obtained by a green machining process even in interrupted cutting. However, to achieve high green machinability, other considerations than cutting parameters must be controlled, such as high green strength as well as density gradients.
- The results indicate that there is a correlation between density gradients, cutting forces and green machinability of P/M compacts. The new technique characterizing density gradients, based on cutting force measurement during green machining, makes it possible to quickly and quantitatively identify density gradients in P/M components. The proposed technique can also be used during press set up to optimize the compaction process and minimize green density gradients. The results of this study highlight a strong relationship between green density gradients and surface finish during green machining. The proposed characterization technique can thus be used to predict the behaviour of P/M components in green machining.
- In terms of green strength, the study shows that the range of values obtained with common lubricant systems, such as ethylenebisstearamide (EBS), is insufficient to allow green machining. Specific binder/lubricant systems must be employed to provide sufficient green strength to the P/M components to make green machining practicable.
- The results indicate that binder/lubricant systems such as the one used in the FLOMET HGS system make green machining a viable process to manufacture high performance sinter-hardenable P/M components. Moreover, performing a curing treatment at 175 °C in air for 1 h increases the green strength of the components to a point where their surface finish after green machining is comparable to that of components machined after sintering.
- For the range of values studied, the optimum cutting parameters usable for the turning of a groove to simulate the machining of a timing sprocket can be summarized as follows:
 - For binder treated components in the as-pressed condition: density of 7.20 g/cm³, surface speed of 152 m/min and feed rate of 0.0254 mm/rev. Average length of breakout land is 315 μm.

- For binder treated components cured at 175 °C in air for 1 h: density of 7.20 g/cm³, surface speed of 305 m/min and feed rate of 0.0254 mm/rev. Average length of breakout land is 220 μm.

Furthermore, since the surface speed has the lowest influence on green machinability, it can be increased without severely affecting the surface finish. In the case of binder treated components cured, if surface speed is increased from 305 to 457 m/min (50% higher), the average length of the breakouts, predicted by the model, increases by only 4%. Thus, this parameter should be maximized for productivity purposes.

References

- [1] D.S. Madan, *Adv. Powder Metall. Part. Mater.* 8 (1995) 55–67.
- [2] R.M. German, *Powder Metallurgy Science*, second ed., Metal Powder Industries Federation, Princeton, 1994.
- [3] A. Benner, P. Beiss, *Adv. Powder Metall. Part. Mater.* 6 (2001) 1–15.
- [4] A. Benner, P. Beiss, *Euro PM2000 Conference on Material and Processing Trends for PM Components in Transportation Proceedings*, Munich, 2000, pp. 101–109.
- [5] M. Ramstedt, O. Andersson, H. Vidarsson, B. Hu, *Adv. Powder Metall. Part. Mater.* 12 (2001) 151–162.
- [6] O. Andersson, A. Benner, *Adv. Powder Metall. Part. Mater.* 6 (2001) 16–28.
- [7] T.M. Cimino, S.H. Luk, *Adv. Powder Metall. Part. Mater.* 8 (1995) 129–148.
- [8] S. St-Laurent, F. Chagnon, *Adv. Powder Metall. Part. Mater.* 3 (1997) 3–18.
- [9] L. Tremblay, J.E. Danaher, F. Chagnon, Y. Thomas, *Adv. Powder Metall. Part. Mater.* 12 (2002) 123–137.
- [10] L. Tremblay, Y. Thomas, *Adv. Powder Metall. Part. Mater.* 2 (1999) 141–156.
- [11] F. Chagnon, L. Tremblay, S. St-Laurent, M. Gagné, *SAE Technical Paper No. 1999-01-0337*, 1999, pp. 71–76.
- [12] L. Tremblay, F. Chagnon, Y. Thomas, M. Gagné, *SAE Technical Paper No. 2001-01-0399*, 2001, pp. 53–61.
- [13] Y. Thomas, K.C. Cole, L. Tremblay, *Adv. Powder Metall. Part. Mater.* 3 (2001) 20–30.
- [14] *ASM Metals Handbook, Powder Metallurgy*, 9th ed., ASM International, vol. 7, 1998, p. 306.
- [15] *ASM Metals Handbook-Desk Edition*, ASM International, 1985, pp. 27–29.
- [16] *Metal Powder Industries Federation, Standards 35*, Princeton, 1998.
- [17] M.S. Phadke, *Quality Engineering Using Robust Design*, Prentice-Hall, Englewood Cliffs, 1989.
- [18] G. Taguchi, *Quality Engineering in Production Systems*, McGraw-Hill, New York, 1989.
- [19] P.J. Ross, *Taguchi Techniques for Quality Engineering*, McGraw-Hill, New York, 1988.
- [20] *Metal Powder Industries Federation, Standards 15*, Princeton, 1998.